

Research Article

Comparisons of three scoring systems based on biparametric magnetic resonance imaging for prediction of clinically significant prostate cancer

Wei Li [☆], Haibing Xu [☆], Wenwen Shang, Guohui Hong ^{*}

Department of Medical Imaging, Jiangsu Vocational College of Medicine, Yancheng, China

ARTICLE INFO

Article history:

Received 27 December 2023

Received in revised form

28 July 2024

Accepted 12 August 2024

Available online 19 August 2024

Keywords:

bpMRI

Diagnosis

Prostate cancer

PI-RADS

Scoring

Purpose: In this study, we aimed to validate and compare three scoring systems based on biparametric magnetic resonance imaging (bpMRI) for the detection of clinically significant prostate cancer (csPCa) in biopsy-naïve patients.

Method: In this study, we included patients who underwent MRI examinations between January 2018 and December 2022, with MRI-targeted fusion biopsy (MRGB) as the reference standard. The MRI findings were categorized using three bpMRI-based scorings, in all of them the diffusion-weighted imaging (DWI) was the dominant sequence for peripheral zone (PZ) and T2-weighted imaging (T2WI) was the dominant sequence for transition zone (TZ). We also used the Prostate Imaging Reporting and Data System version (PI-RADS) v2.1 to evaluate each lesion. For each scoring, we calculated the sensitivity, specificity, negative predictive value (NPV), positive predictive value (PPV), and area under the receiver operating characteristic (ROC) curves (AUC).

Results: The calculated AUC for three bpMRI-based scorings were 83.2% (95% CI 78.8%–87.6%), 85.0% (95% CI 80.8%–89.3%), 82.9% (95% CI 78.4%–87.5%), and 86.0% (95% CI 81.8%–90.1%), respectively. Scoring 2 exhibited significantly superior performance than scoring 1 ($P = 0.01$) and scoring 3 ($P < 0.001$). Moreover, the accuracy of scoring 2 was not decreased significantly as compared to PI-RADS v2.1 ($P = 0.05$). There was no significant difference between 3 bpMRI-based scorings and with PI-RADS in TZ. However, although scoring 2 yielded the highest AUC, it was still notably inferior to PI-RADS ($P = 0.02$).

Conclusion: All three bpMRI-based scorings demonstrated favorable diagnostic accuracy, and scoring 2 performed significantly better than the other two bpMRI-based scorings. Notably, scoring 2 was not significantly inferior to the full-sequence PI-RADS v2.1 in terms of sensitivity and specificity.

© 2024 The Asian Pacific Prostate Society. Published by Elsevier B.V. This is an open access article under the CC BY-NC-ND license (<http://creativecommons.org/licenses/by-nc-nd/4.0/>).

1. Introduction

MRI has become a pivotal imaging technique in the localization, diagnosis, and staging of PCa.^{1,2} In addition, MRGB has been demonstrated to outperform systematic biopsy, substantially reducing the risk of unnecessary diagnosis of insignificant tumors.³ In 2019, the American College of Radiology and the European Society of Urogenital Radiology released the PI-RADS 2.1, with the primary aim of improving the inter-reader agreement on TZ lesions.⁴ According to PI-RADS, the MRI examinations comprise all multiparametric protocols, including T1-weighted imaging (T1WI),

T2WI, dynamic contrast-enhanced (DCE) images, and diffusion-weighted imaging (DWI).^{5,6} Nevertheless, a number of published studies have demonstrated that DCE plays a subordinate role in the TZ and can be ignored for PZ lesions.^{7–9} Consequently, the concept of bpMRI, which excludes DCE, has garnered substantial attention. This approach offers the advantage of significantly reducing image acquisition time and examination costs while maintaining sufficient diagnostic accuracy compared to mpMRI.^{10–13}

Nevertheless, some studies have reported a significant decrease in sensitivity with bpMRI compared to mpMRI, despite higher specificity.^{10,14} Moreover, the scoring using bpMRI without DCE is varied among studies and lacks standardization. In some studies, the final score of a lesion was determined by a single sequence (T2WI is dominant for TZ whereas DWI is dominant for PZ), while in other studies the score was determined by the combination of two sequences.^{7,9,14–16} Several simplified or revised scorings derived from PI-RADS have been proposed up to date. However, these bpMRI-based scorings have not been compared with each

^{*} Corresponding author. Department of Medical Imaging, Jiangsu Vocational College of Medicine, Yancheng, China.

E-mail addresses: contribute_sci@126.com (W. Li), 11368@jsmc.edu.cn (H. Xu), leevie@126.com (W. Shang), hfsj2000@126.com (G. Hong).

[☆] Wei Li and Haibing Xu contributed equally to this study.

other directly, or have not been validated externally. Therefore, in this study we aimed to compare the diagnostic performance of 3 scorings based on bpMRI with each other; moreover, we would compare these scorings with the PI-RADS v2.1.

2. Materials and methods

2.1. Patient selection

This retrospective, single-center study was approved by the Institutional Review Board (IRB), and the requirement of written informed consent was waived. All data were collected in accordance with the Health Insurance Portability and Accountability Act (HIPAA). Within 4 weeks of mpMRI examination, suspicious index lesions underwent MRI-transrectal ultrasonography (TRUS) fusion-guided prostate-targeted biopsy (MRGB). Between January 2018 and December 2022, 401 consecutive males suspected of PCa were identified from electronic databases at our institution. After excluding 77 patients for 1) diagnosed as PCa or treatment prior to MRI examination ($n = 29$); 2) systematic biopsy only ($n = 14$); and 3) severe artifacts on MRI images ($n = 34$), a total of 324 patients (mean age 68.75 ± 8.68 years; mean PSA 19.58 ± 22.69 ng/mL) were included in the final study population.

2.2. MRI acquisition and interpretation

All examinations were conducted using a 3.0 T MRI system, with a pelvic 32-channel phased array coil (Ingenia 3.0 T CX Quasar Dual; Philips Medical Systems, Best, The Netherlands). The mpMRI sequences included axial T1-weighted imaging; axial and sagittal turbo spin echo (TSE) T2-weighted imaging, single-shot echoplanar diffusion-weighted imaging, and dynamic contrast enhancement imaging. The apparent diffusion coefficient (ADC) maps were generated from DWI with b values of 0, 100, 1000, and 2000 s/mm^2 . DCE was conducted immediately after patients were injected with contrast agent of gadobutrol (Gadovist, Bayer Schering Pharma) or gadopentetate dimeglumine (Magnevist, Bayer Schering Pharma), at a dose of 0.1 mL/kg (2–3 mL/s) with a power injector, and followed by a 20 mL saline flush. Detailed MRI protocols used for imaging acquisition are provided in Table 1. All MRI images were independently interpreted by two genitourinary radiologists (both with at least five years of experience) according to three bpMRI-based scorings (scoring 1, scoring 2, and scoring 3), who were blinded to the final histopathology results and other clinical information. To minimize memory effect, after at least 4 weeks these lesions were assessed again according to the PI-RADS v2.1 criteria. With scoring 1, the final score was determined as follows: for PZ the final score is decided by the DWI sequence while for TZ T2WI is the dominant sequence, regardless of the DWI score. Regarding scoring 2, T2 replaces the DCE sequence to determine the final score for PZ lesions; however, when DWI = 3 and T2WI ≥ 4 the final score is upgraded to 4. For TZ lesions, the final score is determined using the

T2WI sequence, and lesions with T2WI = 3 are upgraded to 4 only if DWI = 5. With respect to scoring 3, the dominant sequences were DWI for PZ and T2WI for TZ; however, the final score was determined by combining these two sequences. Details on these 3 scorings are summarized in Table 2. All assessments were performed using a PACS workstation, and the final bpMRI score and the PI-RADS was assigned through discussion in case there were discrepancies.

2.3. Prostate biopsy procedure

Lesions suspicious of PCa identified by MRI underwent targeted biopsy within 4 weeks, which was performed by a urologist (with 7 years of experience in prostate biopsy), utilizing an ESAOTE Mylab Twice color Doppler ultrasound device (with a 7.5-MHz transrectal end-fire probe). Identified lesions were annotated on the MRI T2WI by the radiologists, and an arrow was placed pointing to the approximate center of the target, assigning the lesion to the PZ or TZ in view of distinct PI-RADS criteria for PZ and TZ. Targeted biopsy was performed in a transperineal approach while taking at least two cores (axial and sagittal planes) for individual lesion. The biopsy cores were paraffin embedded, which were cut at 2- μ m intervals and stained with hematoxylin–eosin for microscopic evaluation. An expert genitourinary pathologist (with more than 15 years of experience) evaluated the biopsy specimens and assigned each lesion a Gleason score (GS), who was blinded to the MRI findings. Gleason score is composed of a primary grade plus a secondary grade, with higher scores indicating a more aggressive form of prostate cancer. For lesions proven to be PCa with fusion-targeted biopsy, the corresponding International Society of Urological Pathology (ISUP) grade group was assigned: ISUP 1 = GS 3 + 3; ISUP 2 = GS 3 + 4; ISUP 3 = GS 4 + 3; ISUP 4 = GS 4 + 4; ISUP 5 = GS 9–10.¹⁷ In this study, csPCa was defined as GS ≥ 7 (ISUP ≥ 2) and/or extraprostatic extension. The prostate volume was calculated according to the ellipsoid volume formula (transverse width \times transverse length \times longitudinal height $\times 0.52$), the tumor size was calculated on the basis of T2WI.

2.4. Statistical analysis

The sensitivity, specificity, NPV, PPV, and AUC with their 95% CI were calculated for each of three bpMRI-based scorings and PI-RADS. For scoring 1 and scoring 2, a score of ≥ 4 was defined as positive, while for scoring 3 positive was defined as a score of ≥ 7 . The McNemar test was used to compare the difference in sensitivity and specificity between scoring systems. The overall diagnostic performance of balance between sensitivity and specificity was evaluated using the AUC, and differences between scorings were compared with DeLong's test, with the best being defined as the largest one.¹⁸ The inter-reader agreements for each bpMRI-based scoring and PI-RADS were assessed using Cohen's kappa (κ) value which was interpreted as follows: <0.20 , slight; between 0.21 and

Table 1
MRI parameters.

Parameter	T1WI (axial)	T2WI (axial)	T2WI (sagittal)	DWI ^{a)}	DCE
Field of view (mm)	240 \times 240	220 \times 220	220 \times 220	260 \times 260	220 \times 220
Acquisition matrix	276 \times 406	276 \times 240	240 \times 161	104 \times 125	124 \times 121
Repetition time (ms)	566	3000	4978	6000	3
Echo time (ms)	8	100	100	77	1.45
Section thickness, no gaps (mm)	3.0	3.0	3.0	3.0	3.0
Acquisition time	1 min 10 sec	4 min 6 sec	3 min 42 sec	3 min 54 sec	6 min 7 sec

Abbreviations: DCE, dynamic contrast enhanced imaging; DWI, diffusion weighted imaging; T1WI, T1-weighted imaging; T2WI, T2-weighted imaging.

^{a)} DWI performed with b values of 0, 100, 1000, 2000 s/mm^2 .

Table 2
Three scorings based on bpMRI.

Anatomy zone	PZ			TZ		
	DWI (Dominant)	T2WI	Final score	T2WI (Dominant)	DWI	Final score
Scoring 1	1	Any	1	1	Any	1
	2	Any	2	2	≤3	2
	3	Any	3		≥4	3
	4	Any	4	3	≤4	3
	5	Any	5	4	5	4
Scoring 2	1	Any	1	5	Any	5
	2	Any	2	1	Any	1
	3	≤3	3	2	≤3	2
	4	≥4	4	3	≥4	3
	5	Any	4	4	≤4	3
Scoring 3	1	Any	1 + Any	5	Any	5
	2	Any	2 + Any	1	Any	1 + any
	3	Any	3 + Any	2	Any	2 + any
	4	Any	4 + Any	3	Any	3 + any
	5	Any	5 + Any	4	Any	4 + any

Abbreviations: bpMRI, biparametric magnetic resonance imaging; DWI, diffusion-weighted images; PZ, peripheral zone; T2WI, T2 weighted image; TZ, transition zone.

0.40, fair; between 0.41 and 0.60, moderate; between 0.61 and 0.80, substantial; and ≥ 0.81 , almost perfect. All analysis was performed using R statistical software (version 3.6.1).

3. Results

3.1. Patient characteristics

Of the 324 lesions, 175 were located in the PZ and 149 were in the TZ. At targeted biopsy, 104 were diagnosed with csPca (32.1%) and the remaining 220 were non-csPca or benign prostatic hyperplasia (67.9%), [Tables 3](#) and [4](#) summarize the demographic characteristics of included patients.

3.2. Diagnostic performance

The comprehensive diagnostic performance for 4 scoring systems is detailed in [Table 5](#). We performed comparisons of three bpMRI-based scorings with each other in terms of AUC and found that scoring 2 exhibited significantly superior performance compared to scoring 1 ($P = 0.01$) and scoring 3 ($P < 0.001$). Moreover, the diagnostic performance of scoring 2 was not decreased significantly as compared to PI-RADS v2.1 ($P = 0.05$), even though the DCE sequence was omitted ([Fig. 1](#)). When analyzing lesions according to anatomy zone, no significant differences were observed within 3 bpMRI-based scorings and with PI-RADS in TZ. For lesions in PZ, however, although scoring 2 yielded a higher AUC than two others, it was still notably inferior to PI-RADS ($P = 0.02$,

Table 4
Gleason score distribution.

Gleason score	Location	
	PZ	TZ
≤3 + 3	93	127
3 + 4	38	11
4 + 3	17	5
4 + 4	5	1
>4 + 4	22	5

Abbreviations: PZ, peripheral zone; TZ, transition zone.

[Table S1](#)). [Fig. 2](#) shows an example of one lesion categorized by 3 bpMRI scorings. The inter-reader agreement with Cohen's κ value for 3 bpMRI-based scorings were 0.69 (95% CI 0.62–0.69), 0.70 (95% CI 0.67–0.73), and 0.55 (95% CI 0.52–0.60), respectively. None of these 3 scorings differed significantly from PI-RADS, although the latter demonstrated higher inter-reader agreement ($\kappa = 0.72$, 95% CI 0.69–0.77).

In addition to AUC, we compared the sensitivity and specificity among different scorings. Overall, scoring 2 exhibited significantly higher sensitivity than scoring 1 ($P < 0.001$) but was comparable to scoring 3. Nevertheless, the increase in sensitivity was at the cost of reduced specificity, which was significantly lower than scoring 1 ($P = 0.001$) but still substantially higher than scoring 3 ($P = 0.001$). While comparing scoring 2 with PI-RADS, no significant difference was noted either for sensitivity ($P = 0.18$) or specificity ($P = 0.13$).

Regarding the PZ, scoring 2 at cutoff ≥ 4 exhibited identical sensitivity and specificity to scoring 3 at cutoff ≥ 7 . Comparison

Table 3
Characteristics of patients.

Variable	$n = 324$		P
	csPca ($n = 104$)	Non-csPca ($n = 220$) ^{a)}	
Age (years, mean \pm SD)	71.2 \pm 9.0	67.6 \pm 8.3	<0.01
tPSA (ng/mL, median [IQR])	17.55 (11.00–43.25)	9.00 (6.22–16.00)	<0.01
fPSA (ng/mL, median [IQR])	2.10 (1.14–6.22)	1.41 (0.96–2.25)	<0.01
PV (mL, median [IQR])	39.03 (29.83–61.25)	54.00 (36.37–73.25)	<0.01
PSAD (ng/mL/mL, median [IQR])	0.48 (0.27–1.06)	0.17 (0.12–0.29)	0.02

Abbreviations: csPca, clinically significant prostate cancer; fPSA, free prostate-specific antigen; IQR, interquartile range; PSAD, prostate-specific antigen density; PV, prostate volume; SD, standard deviation; tPSA, total prostate-specific antigen.

^{a)} Including Non-csPca and benign lesions.

Table 5
Diagnostic performance for whole gland.

Indicator	Scoring 1 (Cutoff ≥ 4)	Scoring 2 (Cutoff ≥ 4)	Scoring 3 (Cutoff ≥ 7)	PI-RADS 2.1 (Cutoff ≥ 4)
Sensitivity (95% CI)	66.3% (57.3%–75.4%)	85.6% (78.8%–92.3%)	86.5% (80.0%–93.1%)	88.5% (82.3%–94.6%)
Specificity (95% CI)	83.2% (78.2%–88.1%)	77.7% (72.2%–83.2%)	71.8% (65.9%–77.8%)	80.0% (74.7%–85.3%)
PPV (95% CI)	65.1% (56.0%–74.2%)	64.5% (56.5%–72.5%)	59.2% (51.4%–67.0%)	67.6% (59.8%–75.5%)
NPV (95% CI)	83.9% (79.1%–88.8%)	91.9% (88.0%–95.8%)	91.9% (87.8%–95.9%)	93.6% (90.1%–97.1%)
AUC (95% CI)	83.2% (78.8%–87.6%)	85.0% (80.8%–89.3%)	82.9% (78.4%–87.5%)	86.0% (81.8%–90.1%)
True positive	69/104	89/104	90/104	92/104
True negative	183/220	171/220	158/220	176/220

Abbreviations: AUC, area under the receiver operating characteristic curve; CI, confidence interval; NPV, negative predictive value; PPV, positive predictive value.

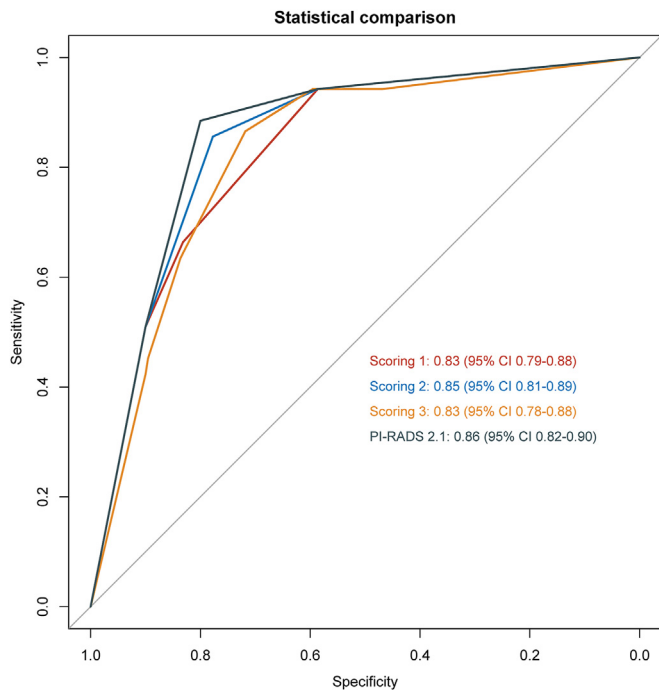


Figure 1. Area under the receiver operating characteristic curve for 4 scoring systems. PI-RADS, Prostate Imaging Reporting and Data System.

between scoring 2 and scoring 1 (cutoff ≥ 4) yielded similar results with the whole gland, that the former generated significantly higher sensitivity ($P < 0.001$) but lower specificity ($P = 0.001$). In comparison with PI-RADS, scoring 2 generated significantly lower specificity ($P = 0.02$) but comparable sensitivity ($P = 0.56$). For the TZ, comparisons indicated minor differences between scorings as compared to PZ. Specifically, scoring 2 had identical sensitivity and specificity with scoring 1, and there was no significant difference compared to PI-RADS ($P = 0.16$ for both sensitivity and specificity). However, scoring 2 showed substantially higher specificity than scoring 3 ($P < 0.001$).

4. Discussion

In this study, we assessed three bpMRI-based scorings and PI-RADS for the prediction of csPCa. Our findings indicated that all of these scoring systems generated favorable diagnostic performance, with AUC of 0.83, 0.85, 0.83, and 0.86, respectively. Furthermore, scoring 1 and scoring 2 showed substantial inter-reader agreement between radiologists ($\kappa = 0.69$ and $\kappa = 0.70$, respectively). However, comparative analyses among these four scorings revealed that scoring 2 significantly outperformed scoring 1 and scoring 3. Moreover, our analysis demonstrated that scoring 2

was not statistically inferior to the PI-RADS v2.1, which utilized a full sequence of mpMRI. While analyzed according to the anatomy zone, no significant difference was found among these scorings for TZ. Regarding PZ, however, although scoring 2 exhibited a higher AUC than the other two bpMRI-based scorings, it was still notably inferior to PI-RADS. We further analyzed the differences in terms of sensitivity and specificity, and the results demonstrated that no significant difference between scoring 2 and PI-RADS for the whole gland. Nevertheless, a significant reduction in specificity was noted in PZ lesions.

The study highlights the significance of considering the diagnostic performance of bpMRI, which excludes the DCE sequence. This omission is often motivated by eliminating the need for intravenous contrast media and reducing examination time (up to 15 minute).¹⁹ Several meta-analyses demonstrated that bpMRI has similar diagnostic accuracy as compared to mpMRI and the DCE was not necessary or secondary, especially for PZ lesions.^{10,12,13} In an earlier meta-analysis including 10 head-to-head studies, the pooled results showed that mpMRI had significantly higher sensitivity (0.85) than did bpMRI (0.80, $P = 0.01$), while no significant difference was found in specificity.¹⁰ Nevertheless, Greer et al demonstrated that although DCE could improve the cancer detection rate of PI-RADS 2, 3, and 4 lesions in PZ, a high rate of DCE positivity may lead to higher false-positive rate.⁸ In a recent meta-analysis, the pooled sensitivity and specificity from 17 bpMRI studies for csPCa were 0.83 and 0.71, respectively.¹² By contrast, our study yielded higher sensitivity and specificity, which could avoid more unnecessary biopsies. However, the head-to-head comparison between bpMRI and PI-RADS in our study showed that without DCE, more lesions (8/175) with GS $\leq 3 + 3$ were referred to biopsy, all of which were located in PZ and were scored 3 with PI-RADS criteria. Previous studies also showed score 3 in the PZ is less likely to be upgraded with bpMRI due to lack of DCE.^{20–22} Nonetheless, some studies reported that results from experienced radiologists were more accurate than those with less experience.¹² In the current study, all MRI images were interpreted by two radiologists with experience of more than 5 years, this may be why we did not observe a significant decrease in sensitivity while omitting the DCE sequence.

Despite that bpMRI is emerging strongly as an alternative tool to mpMRI in the detection, localization, and management of PCa, the application of bpMRI in clinical practice is limited by the lack of a standardized scoring system. Some studies have replaced the DCE with T2WI,^{16,23,24} while others suggested completely disregarding the DCE sequence.^{9,15} In the absence of consensus, there have been diverse approaches to assigning final scores to lesions. In the study of Boesen et al, the final score of PZ lesions was merely dependent on DWI findings, and indeterminate lesions (score 3) were not upgraded to score 4 even without positive DCE findings.^{9,15} However, De Visschere et al, recommended using T2WI as a complement (≤ 3 or ≥ 4) for DWI score 3 lesions in PZ, and DWI score ≤ 4 or $= 5$ were used to help determine the final score for T2WI score 3

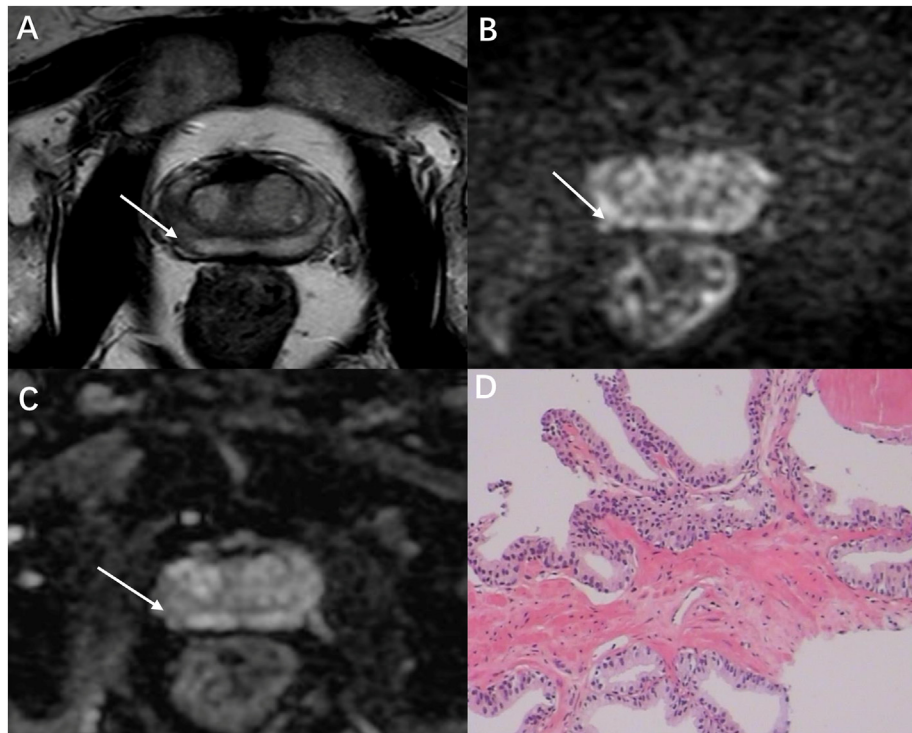


Figure 2. A 63-year-old man with elevated PSA of 11.1 ng/mL and PSAD of 0.27 ng/mL. (A) A marked focal lesion (white arrow) of 11 mm in the right of the PZ with low signal intensity on T2WI; (B) high signal intensity on high b-value image of the DWI; (C) on the ADC map, which showed hypointense; (D) histopathologic image, Gleason score of 4 + 4 at biopsy. This lesion was assigned as score 3, 4, and 7 according to Scoring 1, Scoring 2, and Scoring 3, respectively.

lesions in TZ.⁷ In another study, Scialpi et. al. suggested using a volume of 0.5 cm³ as the cutoff value to manage score 3 lesions, in which category 3a includes lesions with a volume ≤ 0.5 cm³ then are referred to clinical surveillance, whereas category 3b includes lesions with a volume ≥ 0.5 cm³ then are referred to targeted biopsy.¹⁶ In daily clinical practice, the adoption of simplified scoring should facilitate multidisciplinary cooperation and improve the management of suspected PCa.

There are some limitations to the present study. First, this was a single-center retrospective study which may introduced patient selection bias. Therefore, the results and conclusions need to be validated in prospective multi-center studies with a larger number of patients. Second, the use of MRI-TRUS fusion targeted biopsy as the reference standard may miss some undetected PCa lesions, thus the true rate of false-negative readings cannot be assessed. However, all study participants underwent standard biopsies, including those with low-suspicion bpMRI findings. Third, the definition of clinically significant PCa has varied among studies and there has been no consensus currently, which may have led to unreliable conclusions in our study. Finally, the results of our study were from experienced readers, and further validation may be necessary for radiologists with less experience.

5. Conclusion

In this study, we compared three standardized bpMRI-based scorings with each other and with PI-RADS v2.1. The findings indicate that all scorings achieved favorite diagnostic accuracy, and scoring 2 performed significantly better than the other two bpMRI-based scorings. Notably, scoring 2 was not significantly inferior to the full-sequence PI-RADS v2.1 in terms of sensitivity and specificity. Further research, including prospective multicenter studies,

is warranted to validate these findings and establish standardized scoring systems for bpMRI.

Ethics approval and consent to participate

Not applicable.

Funding

Not applicable.

Consent for publication

Patients' data were anonymized. Written informed consent was waived by the Institutional Review Board.

Availability of data and materials

The data that support the findings of this study are available from the corresponding author upon reasonable request.

Conflicts of interest

The authors declare no conflict of interest.

Appendix A. Supplementary data

Supplementary data to this article can be found online at <https://doi.org/10.1016/j.pnrl.2024.08.002>.

References

1. Hoeks CMA, Barentsz JO, Hambrock T, Yakar D, Somford DM, Heijmink SWTPJ, et al. Prostate cancer: multiparametric MR imaging for detection, localization,

- and staging. *Radiology* 2011;261:46–66. <https://doi.org/10.1148/radiol.11091822>.
2. Sandhu S, Moore CM, Chiong E, Beltran H, Bristow RG, Williams SG. Prostate cancer. *Lancet* 2021;398:1075–90. [https://doi.org/10.1016/S0140-6736\(21\)00950-8](https://doi.org/10.1016/S0140-6736(21)00950-8).
 3. Ahmed HU, Bosaily AE-S, Brown LC, Gabe R, Kaplan R, Parmar MK, et al. Diagnostic accuracy of multi-parametric MRI and TRUS biopsy in prostate cancer (PROMIS): a paired validating confirmatory study. *Lancet* 2017;389: 815–22. [https://doi.org/10.1016/S0140-6736\(16\)32401-1](https://doi.org/10.1016/S0140-6736(16)32401-1).
 4. Turkbey B, Rosenkrantz AB, Haider MA, Padhani AR, Villeirs G, Macura KJ, et al. Prostate imaging reporting and data system version 2.1: 2019 update of prostate imaging reporting and data system version 2. *Eur Urol* 2019;76: 340–51. <https://doi.org/10.1016/j.eururo.2019.02.033>.
 5. Barentsz JO, Richenberg J, Clements R, Choyke P, Verma S, Villeirs G, et al. ESUR prostate MR guidelines 2012. *Eur Radiol* 2012;22:746–57. <https://doi.org/10.1007/s00330-011-2377-y>.
 6. Rosenkrantz AB, Ginocchio LA, Cornfeld D, Froemming AT, Gupta RT, Turkbey B, et al. Interobserver reproducibility of the PI-RADS version 2 lexicon: a multi-center study of six experienced prostate radiologists. *Radiology* 2016;280: 793–804. <https://doi.org/10.1148/radiol.2016152542>.
 7. De Visschere P, Lumen N, Ost P, Decaestecker K, Pattyn E, Villeirs G. Dynamic contrast-enhanced imaging has limited added value over T2-weighted imaging and diffusion-weighted imaging when using PI-RADSV2 for diagnosis of clinically significant prostate cancer in patients with elevated PSA. *Clin Radiol* 2017;72:23–32. <https://doi.org/10.1016/j.crad.2016.09.011>.
 8. Greer MD, Shih JH, Lay N, Barrett T, Kayat Bittencourt L, Borofsky S, et al. Validation of the dominant sequence paradigm and role of dynamic contrast-enhanced imaging in PI-RADS version 2. *Radiology* 2017;285:859–69. <https://doi.org/10.1148/radiol.2017161316>.
 9. Obmann VC, Pahwa S, Tabayayong W, Jiang Y, O'Connor G, Dastmalchian S, et al. Diagnostic accuracy of a rapid biparametric MRI protocol for detection of histologically proven prostate cancer. *Urology* 2018;122:133–8. <https://doi.org/10.1016/j.urology.2018.08.032>.
 10. Niu X, Chen X, Chen Z, Chen L, Li J, Peng T. Diagnostic performance of biparametric MRI for detection of prostate cancer: a systematic review and meta-analysis. *Am J Roentgenol* 2018;211:369–78. <https://doi.org/10.2214/AJR.17.18946>.
 11. Bass EJ, Pantovic A, Connor M, Gabe R, Padhani AR, Rockall A, et al. A systematic review and meta-analysis of the diagnostic accuracy of biparametric prostate MRI for prostate cancer in men at risk. *Prostate Cancer Prostatic Dis* 2021;24: 596–611. <https://doi.org/10.1038/s41391-020-00298-w>.
 12. Cuocolo R, Verde F, Ponsiglione A, Romeo V, Petretta M, Imbriaco M, et al. Clinically significant prostate cancer detection with biparametric MRI: a systematic review and meta-analysis. *Am J Roentgenol* 2021;216:608–21. <https://doi.org/10.2214/AJR.20.23219>.
 13. Alabousi M, Salameh J-P, Gusenbauer K, Samoilo L, Jafri A, Yu H, et al. Biparametric vs multiparametric prostate magnetic resonance imaging for the detection of prostate cancer in treatment-naïve patients: a diagnostic test accuracy systematic review and meta-analysis. *BJU Int* 2019. <https://doi.org/10.1111/bju.14759>.
 14. Tamada T, Kido A, Yamamoto A, Takeuchi M, Miyaji Y, Moriya T, et al. Comparison of biparametric and multiparametric MRI for clinically significant prostate cancer detection with PI-RADS version 2.1. *J Magn Reson Imaging* 2021;53:283–91. <https://doi.org/10.1002/jmri.27283>.
 15. Boesen L, Nørgaard N, Løgager V, Balslev I, Bisbjerg R, Thestrup K-C, et al. Assessment of the diagnostic accuracy of biparametric magnetic resonance imaging for prostate cancer in biopsy-naïve men: the biparametric MRI for detection of prostate cancer (BIDOC) study. *JAMA Netw Open* 2018;1:e180219. <https://doi.org/10.1001/jamanetworkopen.2018.0219>.
 16. Scialpi M, Aisa MC, D'Andrea A, Martorana E. Simplified prostate imaging reporting and data system for biparametric prostate MRI: a proposal. *AJR Am J Roentgenol* 2018;211:379–82. <https://doi.org/10.2214/AJR.17.19014>.
 17. Epstein JI, Amin MB, Reuter VE, Humphrey PA. Contemporary gleason grading of prostatic carcinoma: an update with discussion on practical issues to implement the 2014 International Society of Urological Pathology (ISUP) consensus conference on Gleason grading of prostatic Carcinoma. *Am J Surg Pathol* 2017;41:e1–7. <https://doi.org/10.1097/PAS.0000000000000820>.
 18. DeLong ER, DeLong DM, Clarke-Pearson DL. Comparing the areas under two or more correlated receiver operating characteristic curves: a nonparametric approach. *Biometrics* 1988;44:837–45.
 19. Sherrer RL, Glaser ZA, Gordetsky JB, Nix JW, Porter KK, Rais-Bahrami S. Comparison of biparametric MRI to full multiparametric MRI for detection of clinically significant prostate cancer. *Prostate Cancer Prostatic Dis* 2019;22: 331–6. <https://doi.org/10.1038/s41391-018-0107-0>.
 20. Choi MH, Kim CK, Lee YJ, Jung SE. Prebiopsy biparametric MRI for clinically significant prostate cancer detection with PI-RADS version 2: a multicenter study. *AJR Am J Roentgenol* 2019;212:839–46. <https://doi.org/10.2214/AJR.18.20498>.
 21. Di Campli E, Delli Pizzi A, Seccia B, Cianci R, d'Annibale M, Colasante A, et al. Diagnostic accuracy of biparametric vs multiparametric MRI in clinically significant prostate cancer: comparison between readers with different experience. *Eur J Radiol* 2018;101:17–23. <https://doi.org/10.1016/j.ejrad.2018.01.028>.
 22. Merisaari H, Jambor I, Ettala O, Boström PJ, Montoya Perez I, Verho J, et al. IMPROD biparametric MRI in men with a clinical suspicion of prostate cancer (IMPROD Trial): sensitivity for prostate cancer detection in correlation with whole-mount prostatectomy sections and implications for focal therapy. *J Magn Reson Imaging* 2019;50:1641–50. <https://doi.org/10.1002/jmri.26727>.
 23. Pan J, Su R, Cao J, Zhao Z, Ren D, Ye S, et al. Modified predictive model and nomogram by incorporating prebiopsy biparametric magnetic resonance imaging with clinical indicators for prostate biopsy decision making. *Front Oncol* 2021;11:740868. <https://doi.org/10.3389/fonc.2021.740868>.
 24. Kuhl CK, Bruhn R, Krämer N, Nebelung S, Heidenreich A, Schrading S. Abbreviated biparametric prostate MR imaging in men with elevated prostate-specific antigen. *Radiology* 2017;285:493–505. <https://doi.org/10.1148/radiol.2017170129>.